CLINICAL AND VACCINE IMMUNOLOGY, June 2007, p. 775–781 Vol. 14, No. 6
1556-6811/07/$08.00+0 doi:10.1128/CVI.00043-07

Evaluation of a Simplified Dual-Platform Flow Cytometric Method for Measurement of Lymphocyte Subsets and T-Cell Maturation Phenotypes in the Population of Nouna, Burkina Faso▽

T. Böhler,[1]* M. von Au,[1] N. Klose,[1] K. Müller,[1] B. Coulibaly,[3] F. Nauwelaers,[4] H. P. Spengler,[4] G. Kynast-Wolf,[2] and H.-G. Kräusslich[1]

Department of Virology[1] and Department of Tropical Medicine and Public Health,[2] Institute of Hygiene, University of Heidelberg, Heidelberg, Germany; Nouna Health Research Centre, Nouna, Burkina Faso[3]; and BD Biosciences, Erembodegem, Belgium[4]

Received 21 January 2007/Returned for modification 1 March 2007/Accepted 22 March 2007

In the context of a larger clinical study in Nouna, Burkina Faso, we evaluated a simplified dual-platform (DP) flow cytometric (FCM) method that allows the determination of major lymphocyte subsets in a single test tube. We compared the phenotyping of lymphocytes with DP FCM and simultaneous measurements with standard single-platform (SP) FCM for samples from 177 individuals. Analysis of the comparative measurements revealed that DP FCM systematically underestimates the proportion of NK cells, overestimates the percentage of $CD3^+$ $CD8^+$ lymphocytes, and yields proportions of B cells and $CD4^+$ T cells comparable with the results from SP FCM. Bland-Altman analysis showed a low bias between both methods and an acceptable precision for percent values of $CD4^+$ T cells (bias ± precision, −1% ± 6%) and $CD8^+$ T cells (−3% ± 6%). The absolute cell numbers of all lymphocyte subpopulations, however, were systematically biased towards lower values being obtained by DP FCM. Reference values for the distribution of T-cell maturation phenotypes in 177 healthy adults were calculated using DP FCM. The mean ± standard deviation (SD) $CD4^+$-to-$CD8^+$ T-cell ratio was 1.61 ± 0.61, the mean percentage ± SD of $CD4^+$ T cells was 42% ± 7%, and that of $CD8^+$ T cells 29% ± 7%. Among $CD4^+$ lymphocytes, 28% ± 7% were classified as central memory ($CD45RA^{low}$ $CCR7^+$), 22% ± 10% as naïve ($CD45RA^{high}$ $CCR7^+$), 45% ± 12% as effector memory ($CD45RA^{low}$ $CCR7^-$); and 5% ± 3% as terminally differentiated effector memory expressing CD45RA ($CD45RA^{high}$ $CCR7^-$). Among $CD8^{bright}$ lymphocytes, 3% ± 2% had a central memory phenotype, 27% ± 13% were naïve, 37% ± 13% had an effector memory phenotype, and 34% ± 12% were terminally differentiated effector memory cells expressing CD45RA.

In the years 2004 and 2005, a population-based study was performed in Nouna, Burkina Faso, in order to generate site- and gender-specific reference values for lymphocyte subsets in healthy adults in the context of an expanding program for prevention of mother-to-child transmission of human immunodeficiency virus type 1 (HIV-1) (17). During that study, single-platform (SP) flow cytometry (FCM) was used (9), a method which is not available to most laboratories in developing countries due to its relatively high cost (7).

Since lymphocyte differentiation and counting by FCM is needed for immunological monitoring of antiretroviral treatment in resource-limited settings and immunological field studies on cohorts of young infants suffering from diseases other than infection with HIV-1 were planned in our research setting, we wanted to use an FCM test which allows the determination of the complete lymphocyte differential. The test should be reliably performed with low volumes of venous and capillary blood and should be resistant against preanalytic errors. It should be as inexpensive as possible and should be run on a simple flow cytometer equipped with only one laser.

In the present study, we evaluated such a simplified dual-platform (DP) FCM method for its clinical use in Nouna. The method allows the determination of (i) the relative distribution of lymphocyte subsets in peripheral blood in a single test tube (T1) using a mixture of fluorochrome-conjugated monoclonal antibodies on a standard three-color flow cytometer, and (ii) the calculation of absolute values by using lymphocyte numbers obtained from a standard hematology analyzer. The results of simultaneous measurements using DP and SP FCM were compared.

In addition, we generated reference values of T-cell maturation phenotypes for healthy adults living in Nouna, Burkina Faso, by using the linear differentiation model of $CD4^+$ and $CD8^+$ T cells which is based on the expression of the long isoform of the common leukocyte antigen CD45RA and the chemokine receptor CCR7 (13). According to this model, $CD45RA^{high}$ $CCR7^+$ naïve T cells ($T_{naïve}$) develop into $CD45RA^{low}$ $CCR7^+$ central memory cells (T_{CM}) upon stimulation with their cognate antigen and may then switch to the $CD45RA^{low}$ $CCR7^-$ effector memory phenotype upon restimulation. Infection with HIV-1 was shown to influence the distribution of these T-cell maturation phenotypes by increasing the percentage of terminally differentiated, $CD45RA^{high}$ $CCR7^-$ $CD4^+$ T cells—a population which is very small in healthy individuals and has not been well characterized (1, 11). Data on the frequencies and absolute numbers of these T-cell subpopulations are not available for populations in sub-Saharan Africa.

* Corresponding author. Mailing address: c/o Department of Virology, University of Heidelberg, Im Neuenheimer Feld 324, D-69120 Heidelberg, Germany. Phone: 49-6221 565002. Fax: 49-6221 565003. E-mail: thomas.boehler@med.uni-heidelberg.de.

▽ Published ahead of print on 18 April 2007.

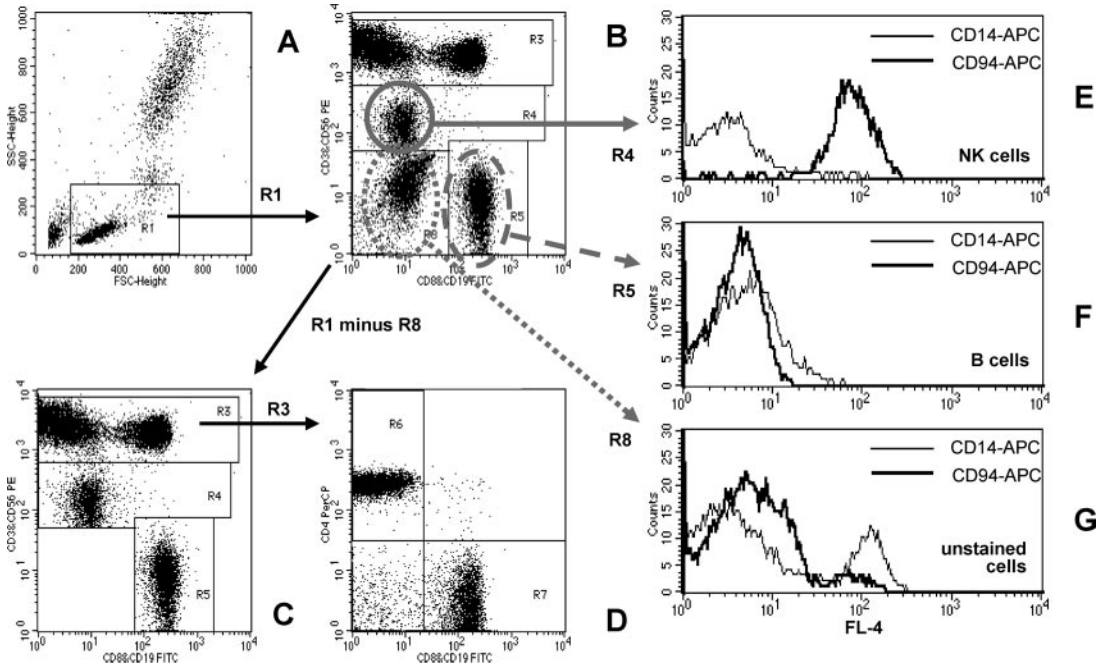

FIG. 1. Quantification of peripheral blood lymphocyte subsets by the T1 FCM method. (A) Lymphocytes are identified as low FSC and low SSC cells (region R1). Details of the gating strategy are described in the text. (B) Region R8 contains cells that did not stain with antibodies against CD3, CD8, CD56, or CD19. This cell population is excluded from analysis by defining the lymphocyte gate G1 for R1 and R2 (R2 includes R3 and R4 and R5 but not R8). (C and D) The dot plots for the final analysis are shown. (E and F) The purity of gating of NK and B cells is shown. (E) The NK cell gate (R1 and R4) contains mainly $CD94^+$ NK cells and very few $CD14^+$ monocytes. (F) Neither $CD94^+$ NK cells nor $CD14^+$ monocytes are found in the B-cell gate (R1 and R5). (G) Cells that did not stain with antibodies against CD3, CD8, CD56, or CD19 include $CD14^+$ monocytes, as well as $CD56^-$ $CD94^+$ NK cells.

MATERIALS AND METHODS

The study took place in northwestern Burkina Faso (West Africa) in the research zone of the Nouna Health Research Center (Centre de la Recherche en Santé de Nouna [CRSN]). From July 2004 until September 2005, the CRSN conducted a population-based clinical study (9), recruiting 364 individuals for the generation of immunohematological reference values in collaboration with the Centre Medical avec Antenne Chirurgicale (CMA) in Nouna, the Institute of Virology at the University of Heidelberg, Germany, and BD Biosciences Europe, Erembodegem, Belgium. The study was part of the ongoing longitudinal prevention of mother-to-child transmission trial in Nouna, which was approved by both the National Ethics Committee in Burkina Faso and the Institutional Ethics Committee of the University of Heidelberg, Germany. The inclusion of healthy adults for the purpose of generating laboratory reference values in the local population was additionally approved by the Institutional Ethics Committee at the Nouna Health Research Center.

In the study presented here, we evaluated a simplified DP FCM method which allows the simultaneous analysis of the major lymphocyte subpopulations in peripheral blood by the T1 method. Measurements using both SP FCM (10) and the simplified DP FCM method were performed for samples from 177 study participants. In addition, reference ranges for lymphocyte subpopulations and T-cell maturation phenotypes were calculated by using complete data sets from 177 healthy adults (68 males and 105 females). Eighteen percent of these individuals were below 20 years of age, 49 percent were between 20 and 29 years of age, 16 percent were between 30 and 39 years of age, and 17 percent were at least 40 years of age.

Details of blood sample collection and serological testing are described elsewhere (9). All FCM measurements were performed on a three-color instrument (BD FACScan) generously provided by BD Biosciences. Standard SP FCM was done with BD MultiSET software, BD TruCount tubes, and BD TriTEST reagents, as recommended by the manufacturer. Hematology testing with an automated device (Sysmex KX21N; Sysmex Corporation, Kobe, Japan) was used to calculate the absolute cell numbers of lymphocyte subpopulations with DP FCM.

Samples for the DP FCM test were prepared at climatized room temperatures (range 20 to 30°C) using a monoclonal antibody reagent mixture as recommended by the manufacturer (tube 1, CD8-fluorescein isothiocyanate [FITC], CD19-FITC, CD56-phycoerythrin [PE], CD3-PE, and CD4-peridin-chlorophyll [PerCP]; tube 2, CD45RA-FITC, CCR7-PE, and CD4-PerCP; tube 3, CD45RA-FITC, CCR7-PE, and CD8-PerCP; and tube 4, immunoglobulin G [IgG] isotype control coupled to FITC, PE, and CD4-PerCP). In preparatory experiments on blood samples from healthy laboratory personnel in Heidelberg, CD8-FITC, CD19-FITC, CD56-PE, CD3-PE, and CD4-PerCP were used in combination with monoclonal antibodies coupled with allophycocyanine (APC) (CD14-APC, CD45-APC, or CD94-APC, respectively) in order to check for purity of the electronic gates and to further characterize lymphocyte subpopulations on a four-color flow cytometer (FACSCalibur; BD). Stained cells were kept in the dark at 2 to 8°C until acquisition on the flow cytometer; measurements were always performed within 12 h of staining.

For the subtyping of lymphocytes with the T1 method, at least 10,000 lymphocytes were acquired by using a forward scatter (FSC)/side scatter (SSC) gate (Fig. 1A). For the determination of T-cell maturation phenotypes on the FACScan flow cytometer, at least 2,500 lymphocytes expressing $CD4^+$ (Fig. 2A) or lymphocytes with a high expression of CD8 (Fig. 2C) were acquired by using an SSC/fluorescence (FL) channel FL-3 gating strategy. The list mode data were analyzed using CellQuest Pro software. In the T1 lymphocyte differential, the T-, B- and natural killer (NK)-lymphocyte subpopulations were identified due to differences in the fluorescence intensities of defined surface antigens and their typical combinations, as shown in Fig. 1A to D.

T-cell maturation phenotypes were defined by the differential expression of the long isoform of the common leukocyte antigen CD45RA and the C-C chemokine receptor CCR7 as originally described by Sallusto et al. (13). $CD4^+$ lymphocytes were identified as low SSC cells with a high FL-3 staining intensity (Fig. 2A) and analyzed in an FL-1 versus FL-2 dot plot (Fig. 2B) for the expression of CD45RA and CCR7. In the $CD8^+$ T-cell subpopulation, maturation phenotypes were determined only in cells expressing high levels of CD8 ($CD8^{bright}$ lymphocytes), in order to exclude $CD8^+$ lymphocytes with intermediate and low CD8 expression. Such cells comprise both NK cells and T cells with NK-like functions; they express only the long isoform of the CD45 antigen (CD45RA) and appear not to participate in the dynamic maturation pathway seen in $CD8^{bright}$ lymphocytes, which are nearly 100% T cells (18).

The markers for the discrimination of the T-lymphocyte maturation pheno-

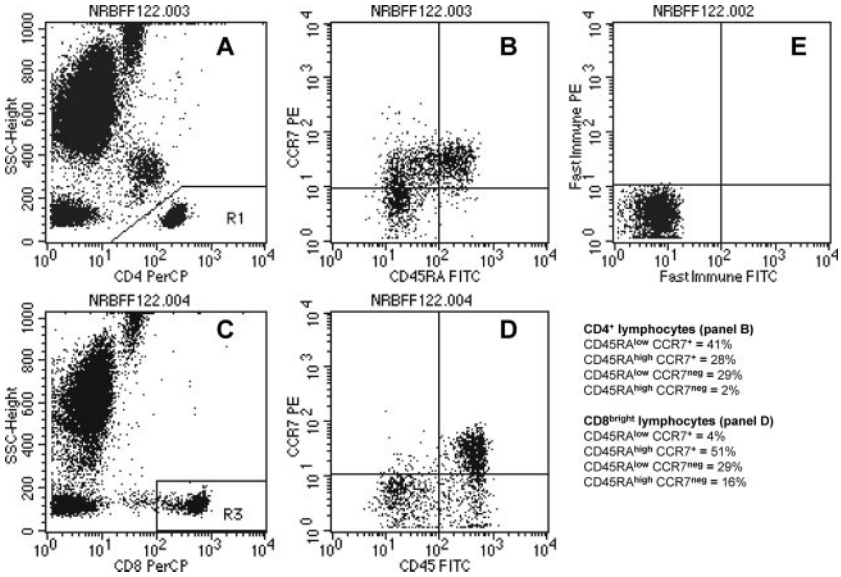

FIG. 2. T-lymphocyte maturation phenotypes. (A) $CD4^+$ lymphocytes are identified as low SSC cells with a high staining intensity in the FL-3 channel (CD4 PerCP). (B) At least 2,500 events in the $CD4^+$ lymphocyte gate were analyzed for the expression of CD45RA and CCR7: upper right, naïve ($CD45RA^{high}$ $CCR7^+$), upper left, central memory ($CD45RA^{low}$ $CCR7^+$), lower left, effector memory ($CD45RA^{low}$ $CCR7^-$), and lower right, terminally differentiated effector memory expressing CD45RA ($CD45RA^{high}$ $CCR7^-$); a typical distribution pattern is displayed. (C) $CD8^{bright}$ lymphocytes were identified as low SSC cells with a fluorescence intensity above 100 arbitrary units in the FL-3 channel (CD8 PerCP). (D) At least 2,500 events in the $CD8^{bright}$ lymphocyte gate were analyzed for the expression of CD45RA and CCR7; a typical distribution pattern is displayed. (E) Markers for the discrimination of T lymphocyte maturation phenotypes were set using a highly purified mouse IgG isotype control to define the boundary between $CCR7^+$ (upper left and upper right quadrants in panels B, D, and E) and $CCR7^-$ (lower left and lower right quadrants). The boundary on the FL-1 axis was fixed at 100 arbitrary fluorescence units in order to identify cells with high CD45RA staining intensities (upper right and lower right quadrants). The quadrant statistics yield the percentages of the T-cell maturation phenotypes for $CD4^+$ (B) and $CD8^{bright}$ (D) lymphocytes.

types were set using mouse IgG isotype control antibodies to define the boundary between $CCR7^+$ and $CCR7^-$ cells. The boundary on the FL-1 axis was fixed at 100 arbitrary fluorescence units in order to clearly distinguish cells with high expression of CD45RA ($CD45RA^{high}$) from cells with low CD45RA staining intensity. Thus, the upper right quadrant in Fig. 2B shows naïve $CD4^+$ lymphocytes ($CD45RA^{high}$ $CCR7^+$), the upper left quadrant the central memory subpopulation ($CD45RA^{low}$ $CCR7^+$), the lower left quadrant effector memory cells (T_{EM}) ($CD45RA^{low}$ $CCR7^-$), and the lower right quadrant terminally differentiated effector memory cells expressing CD45RA (T_{EMRA}) ($CD45RA^{high}$ $CCR7^-$). $CD8^{bright}$ lymphocytes were identified as low SSC cells with a fluorescence intensity above 100 arbitrary units in the FL-3 channel (Fig. 2C) and analyzed as described before (Fig. 2D).

The calculation of reference ranges (5th and 95th percentiles and arithmetic means and standard deviations [SDs] of all parameters) was performed using SAS for Windows. The comparison of relative and absolute lymphocyte counts obtained by SP and DP FCM was done as described by Bland and Altman (4).

RESULTS

Strengths and weaknesses of the simplified DP FCM method. First, we studied potential limitations of the simplified T1 DP FCM method in blood samples from healthy laboratory personnel by using a four-color flow cytometer (FACSCalibur) in Heidelberg. Figure 1 shows the typical result of such an experiment. An electronic gate (G1; region R1) set on the cell population with low FSC and low SSC characteristics was used to identify peripheral blood lymphocytes (Fig. 1A). The expression of different surface antigens, simultaneously stained with different fluorescence-labeled monoclonal antibodies and analyzed in an FL-1 versus FL-2 dot plot (Fig. 1B), allowed the separation of $CD19^+$ B cells as events with high FL-1 (FITC) signal intensity from $CD3^+$ T cells exhibiting high FL-2 (PE) signal intensity (Fig. 1B and C, regions R5 and R3, respectively). NK cells were identified as $CD56^+$ cells with lower FL-2 intensity than $CD3^+$ T cells (region R4 in Fig. 1B and C).

Region R8 in Fig. 1B contains cells that did not stain with antibodies against CD3, CD8, CD56, or CD19. This cell population was excluded from analysis by electronic gating (region R2 in Fig. 1B). The dot plot used for the final analysis is shown in Fig. 1C. $CD3^+$ T cells were further separated into $CD4^+$ and $CD8^+$ subpopulations in an FL-3 (PerCP) versus FL-1 (FITC) dot plot (Fig. 1D: $CD4^+$ T cells, region R6; $CD8^+$ T cells, region R7). As shown in the histogram in Fig. 1E, nearly all NK cells identified as $CD56^+$ lymphocytes were positive for the NK cell marker CD94; the electronic gate (G4; R1 and R4) contained only very few $CD14^+$ monocytes. Contamination of the B-cell gate (G5; R1 and R5) by $CD14^+$ monocytes or $CD94^+$ NK cells was also minimal (Fig. 1F). Thus, the gate purity for the detection of NK cells and B cells was high. However, the use of CD56 as the only NK cell marker led to the loss of specific NK cell subsets from analysis. As shown in Fig. 1G, unstained cells in region R8 comprised both $CD14^+$ monocytes and $CD94^+$ NK cells (electronic gate G8; region R1 and region R8).

When unlysed erythrocytes were added to the measurement tubes, these erythrocytes appeared in the lower left part of region R8; they could be electronically excluded and did not disturb the analysis of the lymphocyte subpopulations (data not shown). The results of the lymphocyte subset analysis were also not influenced by increasing numbers of unstained cells in the test tube (data not shown). Thus, the T1 FCM method in

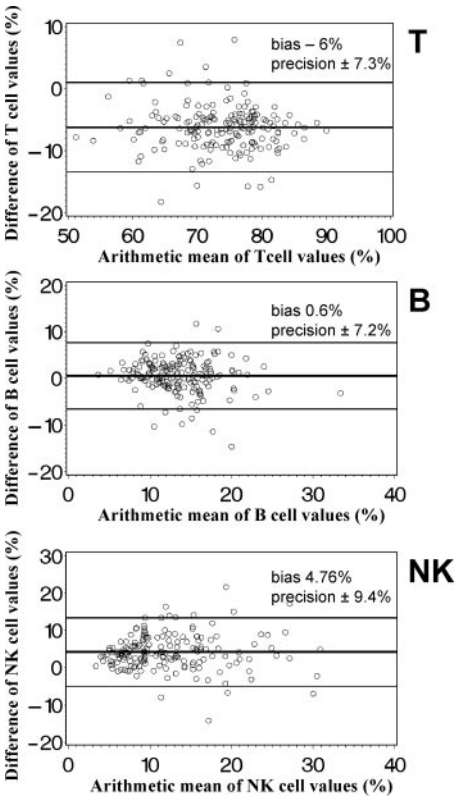

FIG. 3. Bland-Altman diagrams (4) of the relative distribution of T-, B- and NK-lymphocyte subpopulations determined by an SP lyse-no-wash FCM method (MultiSET) and a simplified T1, DP lyse-and-wash method. The arithmetic mean of the lymphocyte percentages (SP FCM plus DP FCM/2) is displayed on the *x* axis, and the difference of the lymphocyte percentages (SP FCM minus DP FCM) on the *y* axis. The horizontal lines indicate the mean difference (bias) ± 2 SD (precision) of simultaneous measurements with both methods of samples from 177 adults.

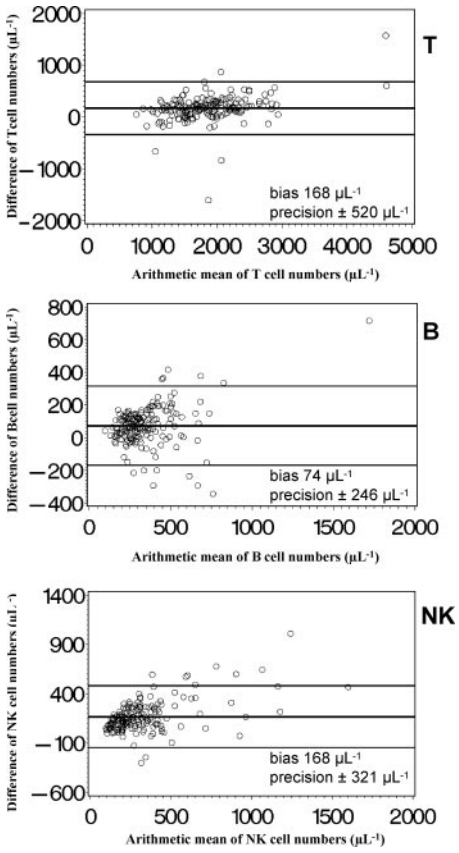

FIG. 4. Bland-Altman diagrams (4) of absolute counts of T-, B- and NK-lymphocyte subpopulations determined by a single-platform lyse-no-wash FCM method (MultiSET) and a simplified T1, DP lyse-and-wash FCM method. The arithmetic mean of the absolute cell counts (SP FCM plus DP FCM/2) is displayed on the *x* axis, and the difference of the absolute cell counts (SP FCM minus DP FCM) on the *y* axis. The horizontal lines indicate the mean difference (bias) ± 2 SD (precision) of simultaneous measurements with both methods of samples from 177 adults.

combination with the electronic gating procedure described here was resistant against typical preanalytic confounders of clinical FCM. The intraindividual coefficients of variation in the distribution of lymphocyte subsets were as follows: 3% $CD3^+$ T cells, 4% $CD4^+$ T cells, 4% $CD8^+$ T cells, 7% $CD19^+$ B cells, and 13% $CD56^+$ NK cells (average results of up to 10 measurements on consecutive days in samples from five healthy individuals).

Methodological comparison of DP and SP FCM. We then applied the simplified DP FCM method in a field study of blood samples from 177 healthy adults in Burkina Faso and observed the following distribution of the lymphocyte differential (mean ± SD): $CD3^+$ T cells represented the most abundant subpopulation (77% ± 8%), followed by $CD19^+$ B cells (13% ± 5%) and $CD56^+$ NK cells (10% ± 6%). The mean $CD4^+$-to-$CD8^+$ T-cell ratio was 1.61 ± 0.61, the mean frequency of $CD4^+$ T cells 42% ± 7%, and that of $CD8^+$ T cells 29% ± 7%. The absolute number of $CD3^+$ T cells was 1,799 ± 537 μl^{-1}, of $CD19^+$ B cells 316 ± 168 μl^{-1}, and of $CD56^+$ NK cells 238 ± 186 μl^{-1}. The mean $CD4^+$ T-cell counts were 980 ± 293 μl^{-1} and the mean $CD8^+$ T-cell counts were 676 ± 300 μl^{-1}.

In order to examine whether the DP FCM method and the standard SP FCM method agreed sufficiently to be regarded as interchangeable, we analyzed data on simultaneous measurements with both methods according to Bland and Altman (4). Both the simplified DP FCM method and the standard SP FCM method gave nearly identical percentages of B cells, while percentages of T cells were higher by DP FCM than by SP FCM and percentages of NK cells were lower (Fig. 3). The absolute numbers of these lymphocyte subpopulations (Fig. 4) were higher if measured by SP FCM than by DP FCM. The bias for T cells was about 10% of the average T-cell number, for B cells about 20% of the average B-cell number, and for NK cells about 50% of the average NK cell number. Thus, the mean bias of absolute cell numbers of these lymphocyte subpopulations was clinically relevant.

Figure 5 illustrates the comparison between the percent values and absolute numbers of $CD4^+$ T cells (Fig. 5A and B) and $CD8^+$ T cells (Fig. 5C and D) generated with the two FCM methods. Bland-Altman analysis indicates that both methods gave nearly identical percentages of $CD4^+$ T cells, while the percentages of $CD8^+$ T cells were higher if measured by DP FCM. The absolute numbers of both T-cell subpopula-

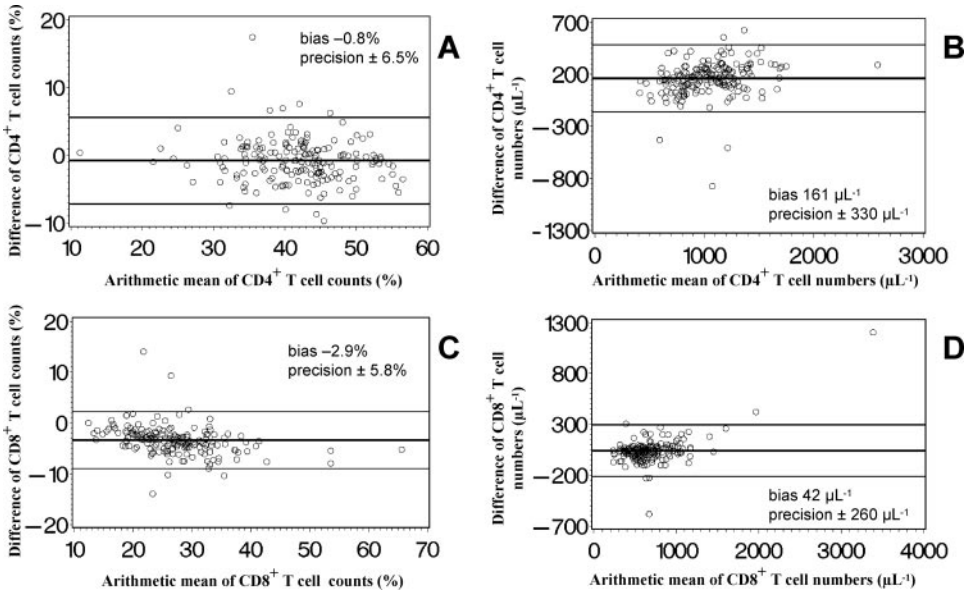

FIG. 5. Bland-Altman diagrams (4) of the relative distribution and absolute cell counts of $CD4^+$ and $CD8^+$ T lymphocyte subpopulations determined by an SP lyse-no-wash FCM method (MultiSET) and a simplified T1, DP lyse-and-wash FCM method. The arithmetic mean of the lymphocyte percentages or absolute cell counts (SP FCM plus DP FCM/2) is displayed on the *x* axis, and the difference of the lymphocyte percentages or absolute cell counts (SP FCM minus DP FCM) on the *y* axis. The horizontal lines show the mean difference (bias) ± 2 SD (precision) of simultaneous measurements with both methods of samples from 177 adults.

tions measured by SP FCM were higher than those obtained with DP FCM. A comparison of the percent values showed a low bias with an acceptable precision for both $CD4^+$ and $CD8^+$ T cells. The bias in terms of absolute cell numbers was approximately 15% of the average cell number in $CD4^+$ T cells and approximately 5% of the average cell number in $CD8^+$ T cells, thus being clinically relevant.

Reference values for T-cell maturation phenotypes. The reference values of the relative distribution (percentages and absolute numbers) of T-lymphocyte maturation phenotypes obtained from 177 healthy adults living in Nouna, Burkina Faso, are shown in Table 1. The characteristic differences between $CD4^+$ and $CD8^{bright}$ lymphocytes are also illustrated, in Fig. 2.

DISCUSSION

We developed a DP FCM method that allows (i) phenotyping of major lymphocyte subsets by the T1 FCM method and (ii) quantification of lymphocyte subsets by simultaneous determination of lymphocyte numbers with an automated hematology counter. Preparatory experiments and analysis of the comparative measurements between simplified DP and standard SP FCM revealed that DP FCM systematically underestimated the percentage of NK cells, probably because these cells are not completely identified by the exclusive use of CD56 as the sole NK cell marker. It has been shown that human NK cells follow a maturational pathway leading from $CD16^+$ $CD56^-$ precursor cells to mature $CD16^+$ $CD56^+$ and $CD16^-$ $CD56^+$ NK cells (5). NK precursor cells are not detected in the T1 assay. Thus, the use of this assay does not permit the quantification of specific subpopulations, such as NK cell precursors, and is limited to screening for a skewed distribution of major subtypes of lymphocytes.

Additionally, the $CD56^{bright}$ NK cell subset (2) may appear in the T-cell region of the T1 analysis, thereby decreasing the percentage of NK cells and concomitantly increasing the percentage of $CD3^+$ and potentially also of $CD8^+$ T cells. These subpopulations were slightly overestimated by DP FCM in comparison to the results of SP FCM, whereas similar proportions of B cells and of $CD4^+$ T cells were detected with both methods.

Despite these shortcomings, the T1 FCM method seems to be suitable for immunological field studies in developing countries. Miniaturization of the assay allows the measurement to be performed in samples of 25 μl of blood at a price of less than $3. It can be reliably performed by skilled laboratory personnel after a short training even on very low volumes of capillary blood from newborn infants (M. von Au, unpublished results), and it is suitable for immunological screening during infectious diseases (or after vaccinations) even in infants suffering from malnutrition, which may influence the distribution of lymphocyte subpopulations other than $CD4^+$ T-cells. Several inexpensive methods have been developed for $CD4^+$ T-cell counting in developing countries; however, these assays usually do not yield the complete lymphocyte differential count (7).

An FCM method similar to the T1 protocol (lymphogram) was published by Bellido et al. (3). No systematic comparison of the lymphogram method and standard FCM was performed on a larger patient cohort or on samples from healthy controls. Giustolisi et al. (6) compared lymphogram measurements to the results of standard multicolor FCM of lymphocyte samples from patients with suspected leukemia and stated that the

TABLE 1. Reference values of $CD4^+$ and $CD8^{bright}$ lymphocyte subpopulations obtained from healthy adults in Burkina Faso[a]

Lymphocyte subset	Central memory T cells		$T_{naïve}$		T_{EM}		T_{EMRA}	
	%	μl^{-1}	%	μl^{-1}	%	μl^{-1}	%	μl^{-1}
$CD4^+$	28 ± 7 (18–40)	277 ± 104 (126–478)	22 ± 10 (5–41)	228 ± 146 (35–496)	45 ± 12 (26–65)	429 ± 147 (230–686)	5 ± 3 (1–11)	45 ± 36 (8–110)
$CD8^{bright}$	3 ± 2 (1–5)	16 ± 11 (4–34)	27 ± 13 (7–52)	173 ± 103 (36–363)	37 ± 13 (17–61)	255 ± 188 (88–576)	34 ± 12 (16–55)	232 ± 135 (71–498)

[a] Relative (%) and absolute (μl^{-1}) counts of lymphocyte subpopulations from 177 healthy adults (109 female, 68 male) given as the means ± SDs with the lower and upper limits of normal (i.e., 5th and 95th percentiles) shown in parentheses.

results "showed no major discordance." No calculation of the absolute numbers of T, B, and NK cells was attempted.

In our study, we compared not only percentages of lymphocyte subpopulations, but also absolute cell numbers, and found a significant systematic bias, showing that SP FCM constantly yielded higher absolute cell counts than DP FCM. This systematic bias had already been described by Nicholson et al. (10), who found higher absolute cell counts (increased by 5 to 10%) with SP FCM using MultiSET/TruCount methodology than with conventional DP FCM (SimulSET and automated hematology). In our cohort in Nouna, Burkina Faso, the absolute $CD4^+$ T-cell counts obtained with SP FCM were approximately 200 cells μl^{-1} higher than absolute $CD4^+$ T-cell counts obtained with DP FCM (calculated by multiplication of the MultiSET data by percentage of $CD4^+$ T cells and the lymphocyte number simultaneously measured with the Sysmex hematology analyzer) (9). Thus, the observed bias between DP FCM and SP FCM corresponds to values reported in the literature.

In the second part of our study, we used a panel of monoclonal antibodies in addition to the T1 DP FCM method in order to assess the relative distribution of naïve and memory subpopulations of peripheral blood T cells. To our knowledge, this is the first description of T-cell maturation phenotypes in a larger cohort of West African healthy adults which is based upon the expression patterns of CD45RA and CCR7. Among $CD4^+$ lymphocytes, such expression patterns have been previously described for eight healthy controls in the United States (1). In that study, 28% ± 2% (mean ± standard error of the mean) of $CD4^+$ T cells were $T_{naïve}$ ($CD45RA^+$ $CCR7^+$), 59% ± 2% were T_{CM} ($CD45RA^-$ $CCR7^+$), 11% ± 1% were T_{EM} ($CD45RA^-$ $CCR7^-$), and 2% ± 1% were T_{EMRA} ($CD45RA^+$ $CCR7^-$). In another study (11), results for $CD4^+$ T cells from 11 healthy adult volunteers in the United States were reported (median and range): 35% (20 to 50%) of cells were $T_{naïve}$, 49% (15 to 70%) were T_{CM}, 12% (2 to 27%) were T_{EM}, and 2% (0 to 22%) were T_{EMRA}.

When the theoretical model of $CD4^+$ and $CD8^+$ effector and memory T-cell generation was first described (12, 16), the authors made the cautionary comment that the markers used for the discrimination of these T-cell subpopulations are rapidly and transiently modulated upon cell activation and the phenotypic characterization applies only to resting cells, i.e., those that are not engaged in an antigen-driven response (12). Especially for the $CD8^+$ T-cell compartment, it has been shown that both the effector memory and the central memory subsets contain populations at intermediate stages of differentiation which may develop into both directions of the differentiation pathway (15). The method used in our study is more reliable in the $CD4^+$ than in the $CD8^+$ T-cell subset. We focused our study on $CD8^{bright}$ T cells because these cells represent the major $CD8^+$ T-cell subpopulation (>95%). We explicitly excluded $CD8^{dim}$ lymphocytes (representing mainly NK cells and NK T cells) from the analysis of maturation phenotypes by electronic gating. Both $CD8^{dim}$ NK cells and $CD8^{dim}$ T cells express high levels of CD45RA, and their inclusion leads to falsely elevated proportions of the naïve subpopulation. Our gating strategy allows us to exclude these cells (which seem not to participate in the dynamic maturation process of the major $CD4^+$ and $CD8^+$ T-cell subpopulations)

despite the use of a flow cytometer equipped with only a single laser.

Recently, Saule et al. (14) obtained data on the relative distribution of naïve and memory subpopulations of $CD4^+$ and $CD8^+$ T cells in 101 healthy blood donors in France and showed changes in the distribution patterns with advancing age of the donors. When comparing our data with those of Saule et al. (14) for the age range of 20 to 40 years (65% of the Nouna donors were in that age range), the median percentage of $T_{naïve}$ in West African donors was only half of that in European donors, while T_{EM} were nearly twice as numerous ($CD4^+$ $T_{naïve}$, 22% versus 50%; T_{EM}, 44% versus 19%; $CD8^+$ $T_{naïve}$, 26% versus 49%; T_{EM}, 36% versus 17%). In terms of absolute cell numbers, these differences were also impressive ($CD4^+$ $T_{naïve}$, 204 versus 357 cells μl^{-1}; T_{EM}, 405 versus 136 cells μl^{-1}; $CD8^+$ $T_{naïve}$, 151 versus 190 cells μl^{-1}; T_{EM}, 215 versus 72 cells μl^{-1}) (14). $CD4^+$ T cells from European donors of ages above 75 years were 34% $T_{naïve}$ (216 cells μl^{-1}) and 24% T_{EM} (156 cells μl^{-1}), and $CD8^+$ T cells were 12% $T_{naïve}$ (49 cells μl^{-1}) and 27% T_{EM} (84 cells μl^{-1}) (14).

In a study on healthy adults from Wonji, Ethiopia (8), T-cell maturation phenotypes were defined by differential expression of CD45RA and CD27 and the following distribution patterns were observed (median and range): among $CD4^+$ T cells, 20% (5 to 47%) were naïve ($CD45RA^+$ $CD27^+$), 53% (40 to 66%) had a memory phenotype ($CD45RA^-$ $CD27^+$), 21% (9 to 45%) showed an effector memory phenotype ($CD45RA^-$ $CD27^-$), and 1% (0 to 5%) were cytotoxic effector cells ($CD45RA^+$ $CD27^-$). Among $CD8^+$ T cells, 29% (5 to 60%) were naïve ($CD45RA^+$ $CD27^+$), 21% (6 to 48%) had a memory phenotype ($CD45RA^-$ $CD27^+$), 9% (2 to 53%) showed an effector memory phenotype ($CD45RA^-$ $CD27^-$), and 34% (8 to 78%) were cytotoxic effector cells ($CD45RA^+$ $CD27^-$). Compared to healthy controls from Amsterdam, The Netherlands, HIV-negative Ethiopians had significantly reduced naïve and increased effector subsets in both the $CD4^+$ and $CD8^+$ T-cell compartments and increased cytotoxic effector cells in the $CD8^+$ T-cell compartment.

In summary, data from Burkina Faso (our study) and Ethiopia (8) indicate substantial T-cell activation in African adults compared to that in people living in France (14). The distribution pattern of T-cell maturation phenotypes may be a surrogate parameter for environmentally driven immunosenescence. Even compared to Europeans with a chronological age above 75 years, young West Africans showed a skewed distribution of T-cell maturation phenotypes, with higher numbers of T_{EM} and lower numbers of $CD4^+$ $T_{naïve}$.

REFERENCES

1. **Alexander, T. H., G. M. Ortiz, M. F. Wellons, A. Allen, E. J. Grace, B. Schweighardt, J. Brancato, J. K. Sandberg, S. N. Furlan, G. D. Miralles, D. F. Nixon, and J. A. Bartlett.** 2003. Changes in CD4+ T-cell differentiation phenotype during structured treatment interruption in patients with chronic HIV-1 infection. J. Acquir. Immune Defic. Syndr. **34:**475–481.
2. **Batoni, G., S. Esin, F. Favilli, M. Pardini, D. Bottai, G. Maisetta, W. Florio, and M. Campa.** 2005. Human CD56bright and CD56dim natural killer cell subsets respond differentially to direct stimulation with Mycobacterium bovis bacillus Calmette-Guerin. Scand. J. Immunol. **62:**498–506.
3. **Bellido, M., E. Rubiol, J. Ubeda, C. Estivill, O. Lopez, R. Manteiga, and J. F. Nomdedeu.** 1998. Rapid and simple immunophenotypic characterization of lymphocytes using a new test. Haematologica **83:**681–685.
4. **Bland, J. M., and D. G. Altman.** 1986. Statistical methods for assessing agreement between two methods of clinical measurement. Lancet **i**(8476)**:** 307–310.
5. **Gaddy, J., and H. E. Broxmeyer.** 1997. Cord blood CD16+56− cells with low lytic activity are possible precursors of mature natural killer cells. Cell. Immunol. **180:**132–142.
6. **Giustolisi, G. M., A. M. Gruszka-Westwood, R. M. Morilla, and E. Matutes.** 2001. Lymphogram: a rapid flow cytometry method for screening patients with lymphocytosis. Haematologica **86:**1223–1224.
7. **Janossy, G., I. V. Jani, N. J. Bradley, A. Bikoue, T. Pitfield, and D. K. Glencross.** 2002. Affordable CD4(+)-T-cell counting by flow cytometry: CD45 gating for volumetric analysis. Clin. Diagn. Lab. Immunol. **9:**1085–1094.
8. **Kassu, A., A. Tsegaye, B. Petros, D. Wolday, E. Hailu, T. Tilahun, B. Hailu, M. T. Roos, A. L. Fontanet, D. Hamann, and T. F. De Wit.** 2001. Distribution of lymphocyte subsets in healthy human immunodeficiency virus-negative adult Ethiopians from two geographic locales. Clin. Diagn. Lab. Immunol. **8:**1171–1176.
9. **Klose, N., B. Coulibaly, D. M. Tebit, F. Nauwelaers, H. P. Spengler, G. Kynast-Wolf, B. Kouyaté, H.-G. Kräusslich, and T. Böhler.** 2007. Immunohematological reference values for healthy adults in Burkina Faso. Clin. Vaccine Immunol. **6:**782–784.
10. **Nicholson, J. K., D. Stein, T. Mui, R. Mack, M. Hubbard, and T. Denny.** 1997. Evaluation of a method for counting absolute numbers of cells with a flow cytometer. Clin. Diagn. Lab. Immunol. **4:**309–313.
11. **Palmer, B. E., E. Boritz, and C. C. Wilson.** 2004. Effects of sustained HIV-1 plasma viremia on HIV-1 Gag-specific CD4+ T cell maturation and function. J. Immunol. **172:**3337–3347.
12. **Sallusto, F., J. Geginat, and A. Lanzavecchia.** 2004. Central memory and effector memory T cell subsets: function, generation, and maintenance. Annu. Rev. Immunol. **22:**745–763.
13. **Sallusto, F., D. Lenig, R. Forster, M. Lipp, and A. Lanzavecchia.** 1999. Two subsets of memory T lymphocytes with distinct homing potentials and effector functions. Nature **401:**708–712.
14. **Saule, P., J. Trauet, V. Dutriez, V. Lekeux, J. P. Dessaint, and M. Labalette.** 2006. Accumulation of memory T cells from childhood to old age: central and effector memory cells in CD4(+) versus effector memory and terminally differentiated memory cells in CD8(+) compartment. Mech. Ageing Dev. **127:**274–281.
15. **Schwendemann, J., C. Choi, V. Schirrmacher, and P. Beckhove.** 2005. Dynamic differentiation of activated human peripheral blood CD8+ and CD4+ effector memory T cells. J. Immunol. **175:**1433–1439.
16. **Seder, R. A., and R. Ahmed.** 2003. Similarities and differences in CD4+ and CD8+ effector and memory T cell generation. Nat. Immunol. **4:**835–842.
17. **Tebit, D. M., J. Ganame, K. Sathiandee, Y. Nagabila, B. Coulibaly, and H. G. Krausslich.** 2006. Diversity of HIV in rural Burkina Faso. J. Acquir. Immune Defic. Syndr. **43:**144–152.
18. **Winkelstein, A., and A. D. Donnenberg.** 1997. Clinical applications of FCM, p. 381–476. *In* M. S. Leffell, A. D. Donnenberg, and N. R. Rose (ed.), Handbook of human immunology. CRC Press, Boca Raton, FL.